Supporting Information

Theranostic fluorescent agents for Hg^{2+} detection and detoxification treatment

Chao Song[a], Wen Yang[a], Nannan Zhou[a], Rui Qian[a], Yajun Zhang[a], Kaiyan Lou*[a], Rui Wang[a], Wei Wang*[a,b]

[a] Shanghai Key Laboratory of Chemical Biology, School of Pharmacy, and State Key Laboratory of Bioengineering Reactor, East China University of Science and Technology, 130 Meilong Road, Shanghai 200237, China
[b] Department of Chemistry and Chemical Biology, University of New Mexico, Albuquerque, NM 87131-0001, USA

General information: Commercial reagents were used as received, unless otherwise stated. All metal ions were purchased as their perchlorates ($LiClO_4 \cdot 3H_2O$, $NaClO_4$, $KClO_4$, $Ca(ClO_4)_2 \cdot 4H_2O$, $Al(ClO_4)_3 \cdot 9H_2O$, $Cr(ClO_4)_3 \cdot 6H_2O$, $Fe(ClO_4)_3 \cdot H_2O$, $Fe(ClO_4)_2 \cdot 6H_2O$, $Co(ClO_4)_2 \cdot 6H_2O$, $Ni(ClO_4)_2 \cdot 6H_2O$, $Cu(ClO_4)_2 \cdot 6H_2O$, $Zn(ClO_4)_2 \cdot 6H_2O$, $Cd(ClO_4)_2 \cdot 6H_2O$, $Pb(ClO_4)_2 \cdot 3H_2O$, $Hg(ClO_4)_2 \cdot 3H_2O$, and $AgClO_4 \cdot H_2O$), except Cu^+ and Au^+ as chloride (CuCl and AuCl). ^1H and ^{13}C NMR spectra were recorded on Bruker DRX 400 (400 MHz) and Bruker DRX 500 (500 MHz), and tetramethylsilane (TMS) was used as a reference. Data for ^1H are reported as follows: chemical shift (ppm), and multiplicity (s = singlet, d = doublet, t = triplet, q = quartet, m = multiplet). Data for ^{13}C NMR are reported as ppm. High Resolution Mass Spectra were obtained from East China University of Science and Technology mass spectral facility. Single crystal X-ray diffraction analysis was obtained from Analysis and Test Center of Shanghai Institute of Organic Chemistry, Chinese Academy of Science.

Spectroscopic materials and methods: The pH was recorded by a METTLER TOLEDO FE20 pH meter. UV absorption spectra were recorded on a Shimadzu UV-1800 UV-Vis spectrophotometer. Fluorescence spectra were obtained on a Horiba Fluoromax-4 fluorometer equipped with a R928 detector. IR spectra were obtained on a Thermo Scientific Nicolet 6700 FT-IR Spectrometer.

Synthetic procedures:

(2*s*,4*S*,5*R*)-2-(7-(diethylamino)-2-oxo-2*H*-chromen-3-yl)-1,3-dithiolane-4,5-dicarboxylic acid (**1a**)
(2*r*,4*R*,5*S*)-2-(7-(diethylamino)-2-oxo-2*H*-chromen-3-yl)-1,3-dithiolane-4,5-dicarboxylic acid (**1b**)
To a stirred solution of **3**[1] (100 mg, 0.41 mmol) in dry DCM (4 ml) under N_2

atmosphere at 0 ^{o}C, a solution of DMSA (111 mg, 0.61 mmol) in DMF (4 mL) and 256 μL of $BF_3{\cdot}Et_2O$ (2.1 mmol) was added. The reaction mixture was stirred at room temperature for overnight. The solvent was evaporated under reduced pressure. The residue was added 5mL H_2O and extracted twice using EtOAc (5 mL each). The combined organic layer was washed with 1M HCl (5 mL) for three times and brine (10 mL). And then the organic layer was dried over anhydrous Na_2SO_4 and solvent was removed under reduced pressure. The residue was purified via column chromatography (silica gel) using DCM:MeOH:HCOOH = 60:2:1(V/V/V) as the eluent solvent to obtain **1a** (78 mg, 47%) and **1b** (23 mg, 14%) as white solid. Compound **1a**: ^{1}H NMR (400 MHz, DMSO-d_6): δ 13.03 (s, 2H), 8.08 (s, 1H), 7.49 (d, J = 8.9 Hz, 1H), 6.71 (dd, J = 8.9, 2.3 Hz, 1H), 6.55 (d, J = 2.3 Hz, 1H), 5.68 (s, 1H), 4.72 (s, 2H), 3.43 (q, J = 6.9 Hz, 4H), 1.12 (t, J = 6.9 Hz, 6H); ^{13}C NMR (100 MHz, DMSO-d_6): δ 170.0, 160.8, 155.4, 150.7, 140.7, 129.8, 117.2, 109.2, 107.3, 96.3, 55.8, 47.9, 44.1, 12.3. HR-ESI-Mass, (m/z): [M - H^+] calcd. for $C_{18}H_{18}NO_6S_2$: 408.0576, obsd: 408.0570. Compound **1b**: ^{1}H NMR (400 MHz, DMSO-d_6): δ 12.99 (s, 2H), 8.14 (s, 1H), 7.49 (d, J = 8.9 Hz, 1H), 6.71 (dd, J = 8.9, 2.4 Hz, 1H), 6.53 (d, J = 2.4 Hz, 1H), 5.63 (s, 1H), 4.75 (s, 2H), 3.42 (q, J = 6.9 Hz, 4H), 1.11 (t, J = 6.9 Hz, 6H). ^{13}C NMR (100 MHz, DMSO-d_6): δ 170.0, 160.5, 155.4, 150.5, 139.7, 129.8, 119.1, 109.2, 107.4, 96.2, 55.5, 48.4, 44.1, 12.3; HR-ESI-Mass (m/z): [M - H^+] calcd. for $C_{18}H_{20}NO_6S_2$: 408.0576, obsd: 408.0571.

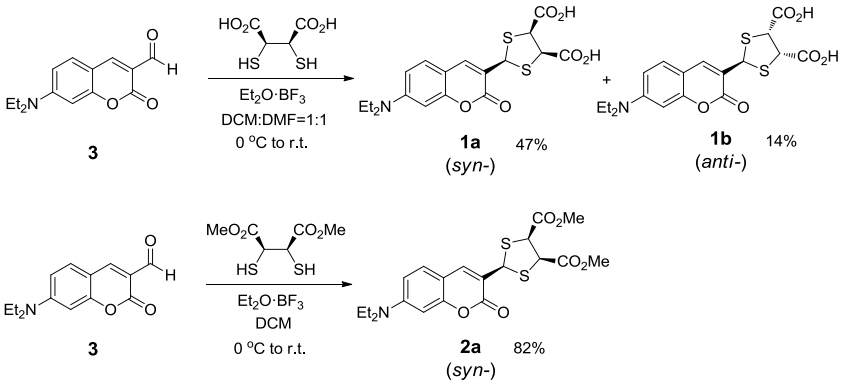

Scheme S1. Synthesis of probe **1a-b** and **2a**

(2*s*,4*S*,5*R*)-dimethyl 2-(7-(diethylamino)-2-oxo-2*H*-chromen-3-yl)-1,3-dithiolane-4,5-di-carboxylate acid (**2a**)

To a stirred solution of **3** (74 mg, 0.30 mmol) in dry DCM (6 ml) under N_2 atmosphere at 0 ^{o}C, a solution of DMSA dimethylester[2] (94.5 mg, 0.45 mmol) and 192 μL of $BF_3{\cdot}Et_2O$ (1.6 mmol) was added. The reaction mixture was stirred for 30 min at room temperature. The solvent was evaporated under reduced pressure. The residue was purified via column chromatography using petroleum ether:DCM:Et_2O = 5:5:1 as eluent to obtain **2a** as white solid (108 mg, 82%). ^{1}H NMR (400 MHz, $CDCl_3$): δ 8.09 (s, 1H), 7.29 (d, J = 8.9 Hz, 1H), 6.71 (dd, J = 8.9, 2.4 Hz, 1H), 6.55 (d, J = 2.4 Hz, 1H), 5.88 (s, 1H), 4.64 (s, 2H), 3.75 (s, 6H), 3.41 (q, J = 7.1 Hz, 4H), 1.20 (t, J = 7.1 Hz, 6H); ^{13}C NMR (100 MHz, $CDCl_3$) δ 169.33, 161.99, 156.04,

151.09, 141.66, 129.47, 117.73, 109.19, 108.37, 97.16, 56.37, 53.09, 48.86, 44.97, 12.55; HR-EI-Mass (m/z): calcd. for $C_{20}H_{23}NO_6S_2$: 439.0967, obsd: 439.0968.

Proposed mechanism for formation of the dithiane ring:

As shown in **Scheme S2**, it was proposed that the dithiane rings were formed via semi-thioacetal intermediates through an intramolecular S_N2 type cyclization with flip of the previous aldehyde carbonyl carbon and retention of stereocenters in DMSA. Therefore, the ratio of products should equal to the ratio of the semi-thioacetal intermediates (**I** and **II**) formed. Since the hydrogen atom is a much smaller group than the carboxylic acid group, formation of the semi-thioacetal intermediate **I** was energetically more favored, which led to the dithiane **1a** as the major product. The same model could also be applied to the formation **2a**. The improved yield of **2a** could be rationalized by increased steric bulkiness of the methyl ester group. The predicted stereochemistry of **1a** and **2a** was supported by 2D-NOESY spectra. Moreover, the structure of **2a** was further confirmed by X-ray crystallography.

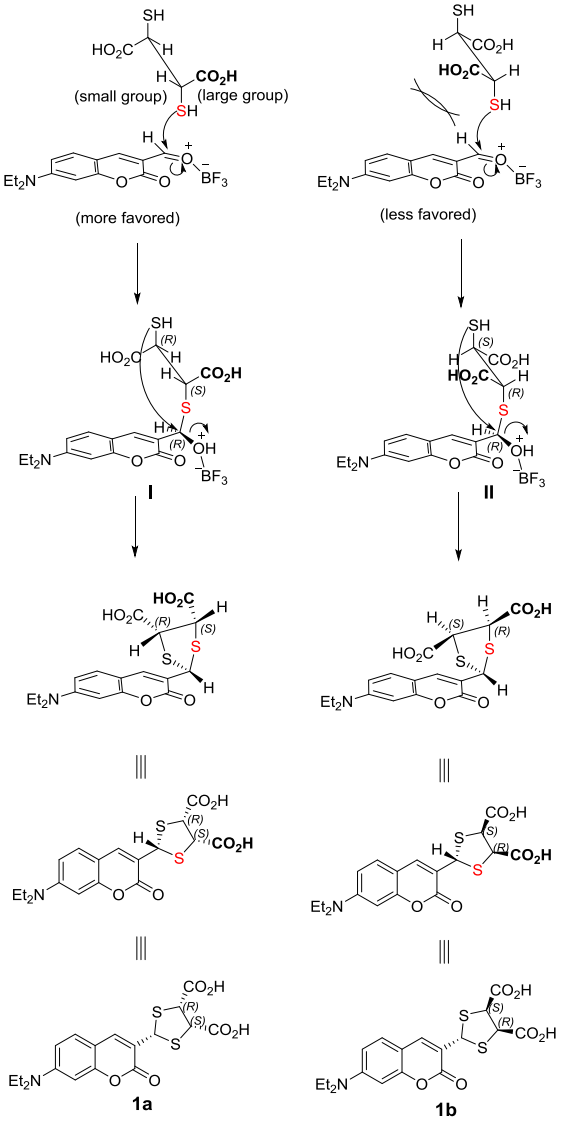

Scheme S2. Proposed mechanism of dithiane formation

Proposed mechanism for Hg^{2+}- assisted hydrolysis of the dithiane ring:

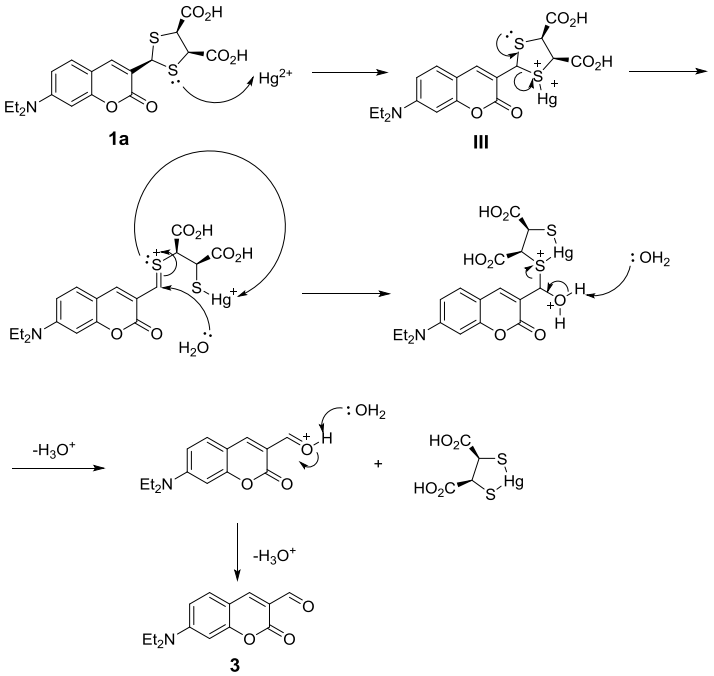

Scheme S3. Proposed mechanism of dethiolation of Hg^{2+} with probe **1a** (^{1}HNMR and IR supporting see Fig. S19 and S20)

Reaction kinetic studies:

Procedure for reaction kinetic measurements was adapted from reported protocol[3] with minor modifications. The second order reaction between each probe and Hg^{2+} was assumed. The reaction of probe **1** or **2a** (2 μM) with 100 equiv. Hg^{2+} were conducted in 0.02 M PBS buffer solution containing 0.2% DMSO at 25 ^oC, and monitored using the fluorescence intensity at 502 nm (excited at 477 nm, 2 nm slit width for both excitation and emission, the excitation and emission wavelength were selected for optimized turn-on fluorescence signal readout of the probe **1a**). The *pseudo*-first-order rate constant (*k*') for each probe was determined by fitting the fluorescence intensities of the sample at different time to the following equation I:

$$Ln[(F_{max}-F_t)/F_{max}] = -k't \qquad \textbf{Equation I}$$

Where F_t and F_{max} are the fluorescence intensities at 502 nm at time t and the maximum value obtained after the reaction was complete, and *k*' is the *pseudo*-first-order rate constant, which is related to the second-order rate constant (*k* in $M^{-1}s^{-1}$) by the following equation II. Thus, the second-order rate constant (*k*) can be calculated from the pseudo-first-order rate constant (*k*') obtained from linear fitting plot based on equation I.

$$k' = k[Hg^{2+}] \qquad \textbf{Equation II}$$

For probe **1a** and **2a**, the *pseudo*-first-order rate constants (*k*') obtained from the negative slop of the linear fitting plots listed below were 0.00355 s^{-1}, and 0.00302 s^{-1} respectively. Thus corresponding second-order rate constants (*k*) for probe **1a** and **2a** towards Hg^{2+} were 17.7 $M^{-1}s^{-1}$ and 15.1 $M^{-1}s^{-1}$, respectively.

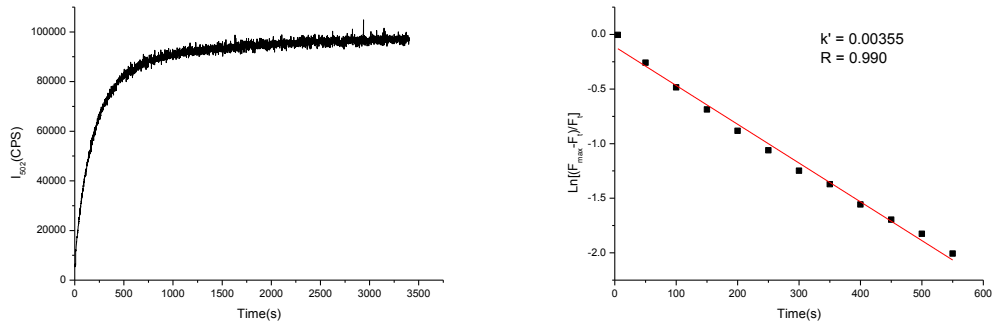

Figure S1. a) The fluorescence intensity of probe **1a** (2 μM) incubated with Hg^{2+} (100 equiv.) at 502 nm for 0-60 min; b) Pseudo first-order kinetic plot of the reaction of **1a** (2 μM) incubated with Hg^{2+} (100 equiv.).

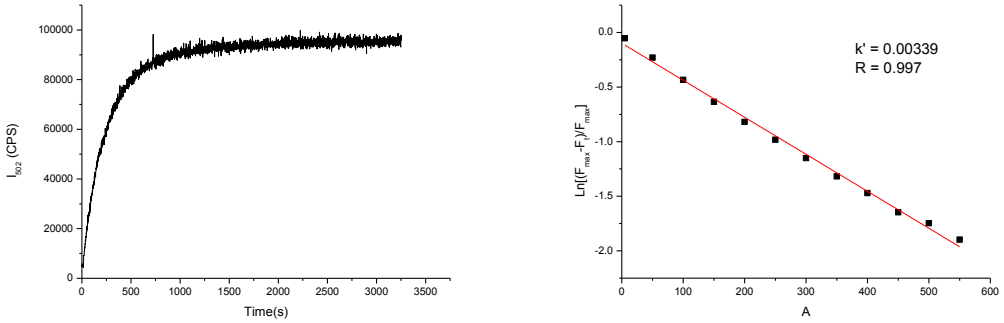

Figure S2. a) The fluorescence intensity of **1b** (2 μM) incubated with Hg^{2+} (100 equiv.) at 502 nm for 0-60 min.

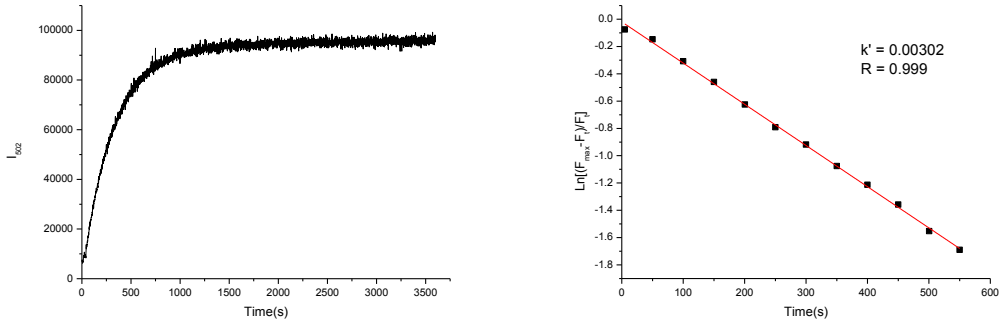

Figure S3. a) The fluorescence intensity of **2a** (2 μM) incubated with Hg^{2+} (100 equiv.) at 502 nm for 0-60 min. b) Pseudo first-order kinetic plot of the reaction of **2a** (2 μM) incubated with Hg^{2+} (100 equiv.).

Determination of reaction stoichiometry of probe 1a:

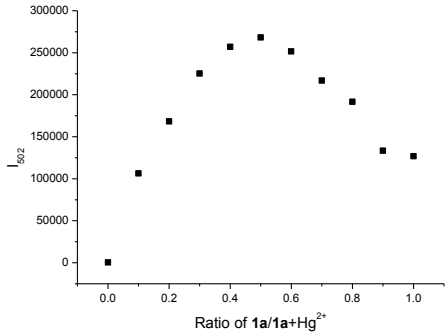

Figure S4. Job's plot of probe **1a** and Hg^{2+}. The total concentration of the probe and Hg^{2+} was kept constant at 10 μM. All measurements were taken in 0.02 M PBS buffer containing 1% DMSO at 25 ^{o}C with incubation time of 15 min.

pH Dependence of probe 1a and Hg^{2+}:

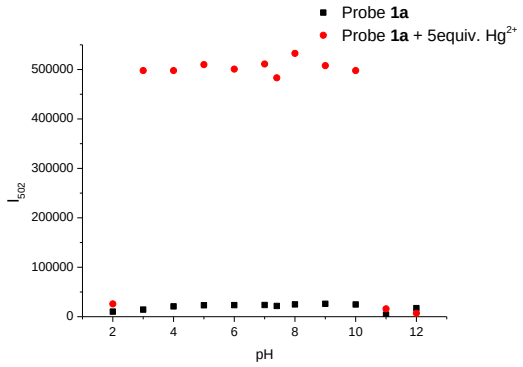

Figure S5. Fluorescence response of probe **1** (2 μM) to 5 equiv. Hg^{2+} at different pHs. All measurements were taken after incubation time of 24 h in 0.02 M PBS buffer solution containing 0.2% DMSO at 25 °C, pHs were adjusted by 1M HCl or 1M NaOH.

Chemodosimeter properties of probe 1a and compound 3 towards Hg^{2+}:

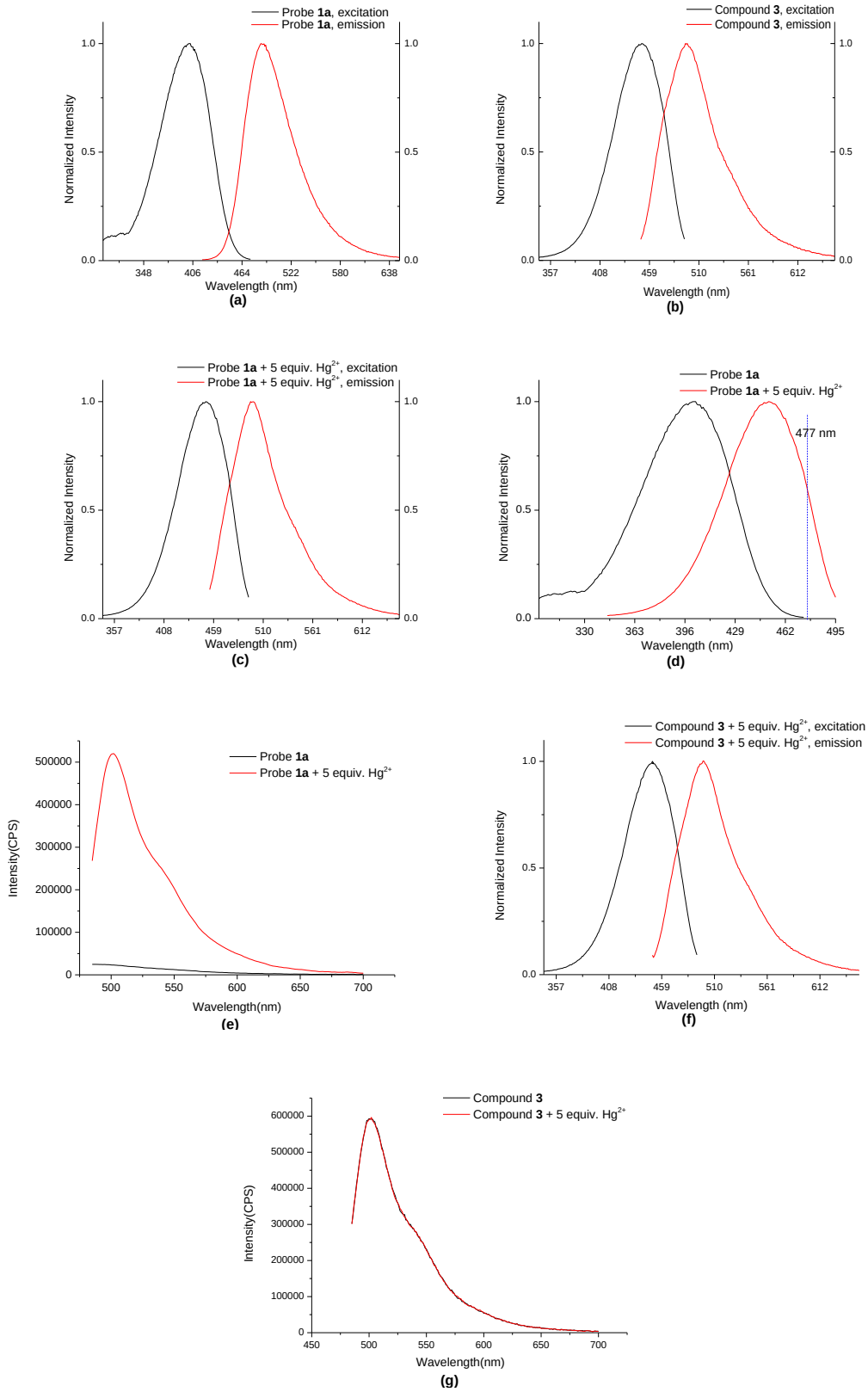

Figure S6. a) Normalized fluorescence excitation (λ_{em} = 488 nm) and emission (λ_{ex} = 403 nm) spectra of probe **1a** (2 μM); b) Normalized fluorescence excitation (λ_{em} =

502 nm) and emission spectra (λ_{ex} = 450 nm) of compound **3** (2 μM) ; c) Normalized fluorescence excitation (λ_{em} = 502 nm) and emission spectra (λ_{ex} = 450 nm) of probe **1a** (2 μM) with 5 equiv. of Hg^{2+}; d) Overlap of normalized fluorescence excitation spectra of the probe **1a** (2 μM) and **1a** with 5 equiv. of Hg^{2+}, from which an optimal excitation wavelength at 477 nm was determined; e) Fluorescence excitation spectra (λ_{ex} = 477 nm) of probe **1a** and probe **1a** with 5 equiv. Hg^{2+}; f) Normalized fluorescence excitation (λ_{em} = 502 nm) and emission spectra (λ_{ex} = 450 nm) of compound **3** (2 μM) with 5 equiv. of Hg^{2+}; g) Fluorescence excitation spectra (λ_{ex} = 477 nm) of compound **3** and compound **3** with 5 equiv. Hg^{2+};. All measurements were taken in 0.02M PBS buffer solution containing 0.2% DMSO (pH = 7.4) at 25 °C with incubation time 60 min and slit width 3 nm for both excitation and emission).

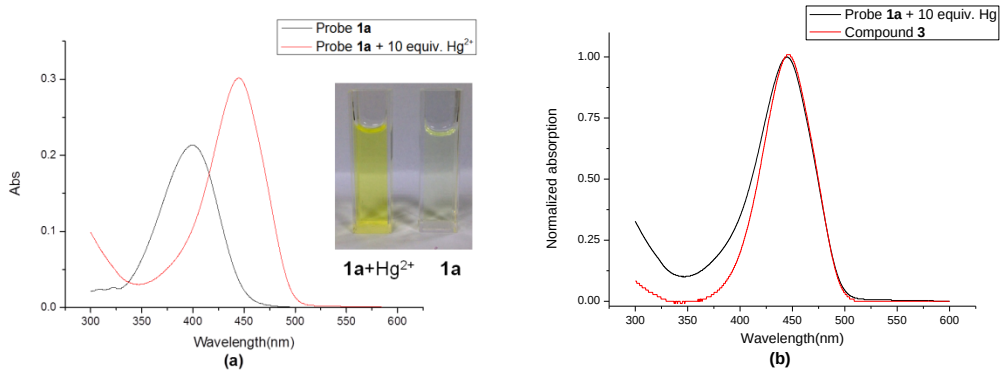

Figure S7. a) UV-Vis spectra of probe **1a** (10 μM, black line) and the probe **1a** at 10 μM with 10 equiv. Hg^{2+} ions (red line); b) Normalized UV-Vis spectra of probe **1a** at 10 μM with 10 equiv. Hg^{2+} ions (black line) and compound **3** (10 μM, red line); All measurements were taken in 0.02 M PBS buffer solution containing 1% DMSO (pH=7.4) at 25 °C with incubation time of 2h.

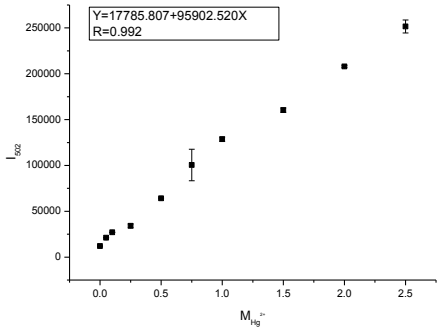

Figure S8. Plot of fluorescence intensity of probe **1a** (1 μM) at different concentrations of Hg^{2+} (0-2.5 μM). All measurements were taken in 0.02 M PBS buffer solution containing 0.1% DMSO at 25 °C with an incubation time of 15 min. (The detection limit was calculated based on the fluorescence titration. The I_{502} of free probe **1a** was collected for 10 times, the S/N ratio and the standard deviation of blank measurements was determined. Under the optimum conditions, a good linear relationship between the fluorescence intensity and the Hg^{2+} concentration could be

obtained in the 0-3.0 μM (R = 0.995). The detection limit is calculated with the equation: detection limit = 3σbi/m, where σbi is the standard deviation of blank measurements; m is the slope between I_{502} versus Hg^{2+} concentration. The detection limit was measured to be 2.4 nM at S/N = 3.)

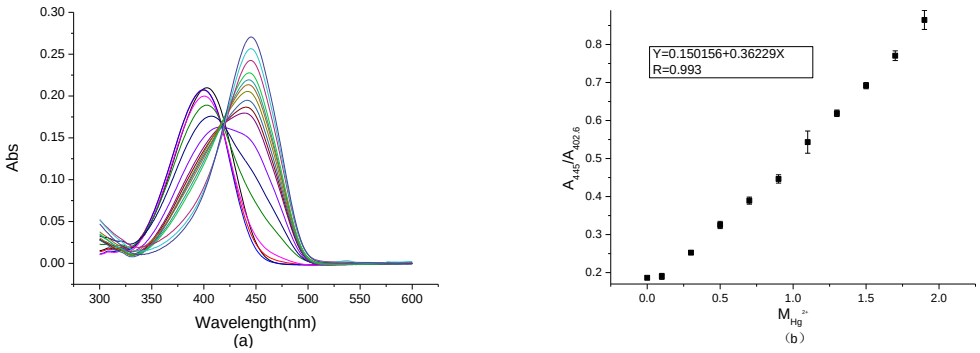

Figure S9. a) UV/Vis spectra of probe **1a** (10.0 μM) at different concentrations of Hg^{2+} (0-10.0 equiv.). All measurements were taken after incubation time of 30 min in 0.02 M PBS buffer solution containing 1% DMSO at 25 °C. b) Plot of A_{445}/A_{403} of probe **1a** (1.0 μM) at different concentration of Hg^{2+} (20 nM - 3.5 μM). All measurements were taken after incubation time of 30 min in 0.02 M PBS buffer solution containing 1% DMSO at 25 °C. (The detection limit was calculated based on the UV/Vis titration. The A_{445}/A_{403} of free probe **1a** was collected for 10 times, the S/N ratio and the standard deviation of blank measurements was determined. Under the optimum conditions, a good linear relationship between the A_{445}/A_{403} and the Hg^{2+} concentration could be obtained in the 0-3.5 μM (R = 0.998). The detection limit is calculated with the equation: detection limit = 3σbi/m, where σbi is the standard deviation of blank measurements; m is the slope between A_{445}/A_{403} versus Hg^{2+} concentration. The detection limit was measured to be 12.0 nM at S/N = 3.)

Selectivity of probe 1a towards Hg^{2+}:

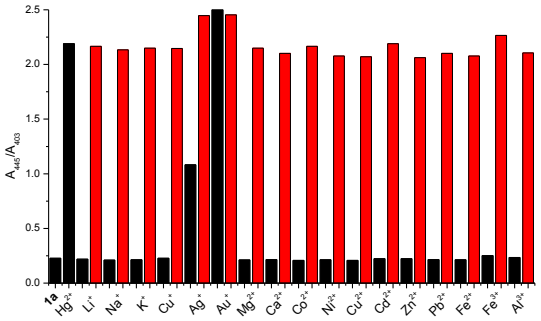

Figure S10. Plot of A_{445}/A_{403} of probe **1a** (10 μM) upon the addition of Li^{+}, Na^{+}, K^{+}, Cu^{+}, Ag^{+}, Au^{+}, Mg^{2+}, Ca^{2+}, Co^{2+}, Fe^{2+}, Cu^{2+}, Zn^{2+}, Cd^{2+}, Pb^{2+}, Cr^{3+}, Fe^{3+}, Al^{3+} (50 equiv., each) and Hg^{2+} (5 equiv., each). Black bars: free probe, or treated with the marked metal ions (50 equiv.). Red bars: treated with the marked metal cations (50

equiv.) followed by Hg^{2+} (5 equiv.). All measurements were taken in 0.02 M PBS buffer solution containing 1% DMSO at 25 °C after incubation time of 30 min.

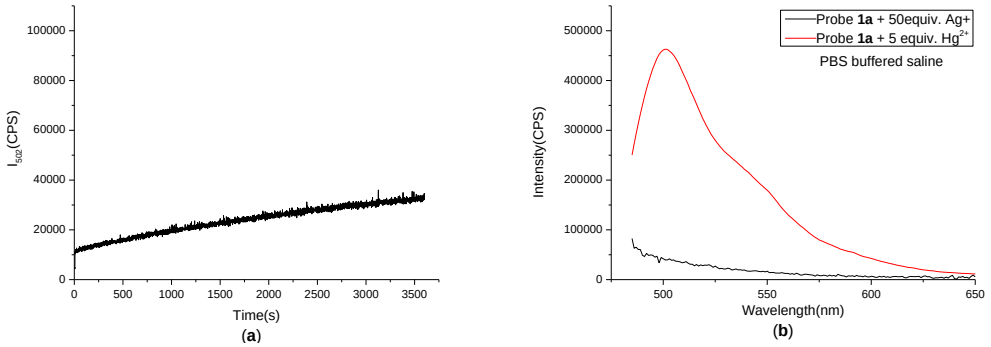

Figure S11. a) The fluorescence intensity of probe **1a** (2 μM) incubated with Ag^{+} (100 equiv.) in 0.02 M PBS buffer containing 0.2% DMSO at 502 nm for 0-60 min (excited at 477 nm, 2 nm slit width for both excitation and emission); b) Fluorescence excitation spectra (λ_{ex} = 477 nm) of probe **1a** (2 μM) with 50 equiv. Ag^{+} and probe **1a** (2 μM) with 5 equiv. Hg^{2+}. All measurements were taken in 0.02 M PBS buffered saline solution containing 0.2% DMSO (pH = 7.4) and 154 mM NaCl at 25 °C. The incubation time was 15 min. Slit width 3 nm for both excitation and emission.

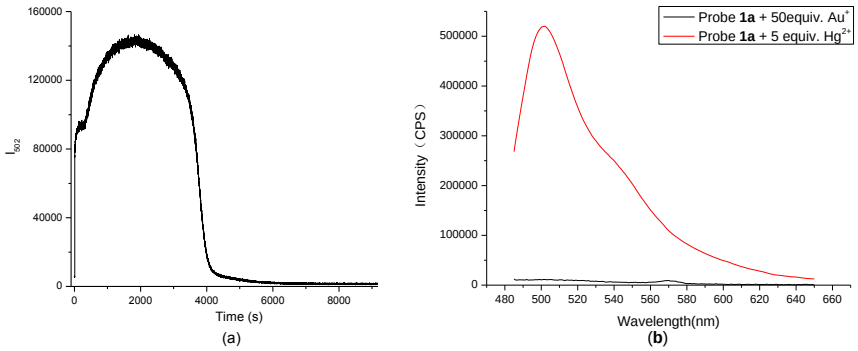

Figure S12. a) The fluorescence intensity of probe **1a** (2 μM) incubated with Au^{+} (100 equiv.) in 0.02 M PBS buffer containing 0.2% DMSO at 502 nm for 0-150 min (excited at 477 nm, 2 nm slit width for both excitation and emission); b) Fluorescence excitation spectra (λ_{ex} = 477 nm) of probe **1a** (2 μM) with 50 equiv. Au^{+} and probe **1a** (2 μM) with 5 equiv. Hg^{2+}. All measurements were taken in 0.02 M PBS buffer containing 0.2% DMSO (pH = 7.4) at 25 °C. The incubation time was 2 h. Slit width 3 nm for both excitation and emission.

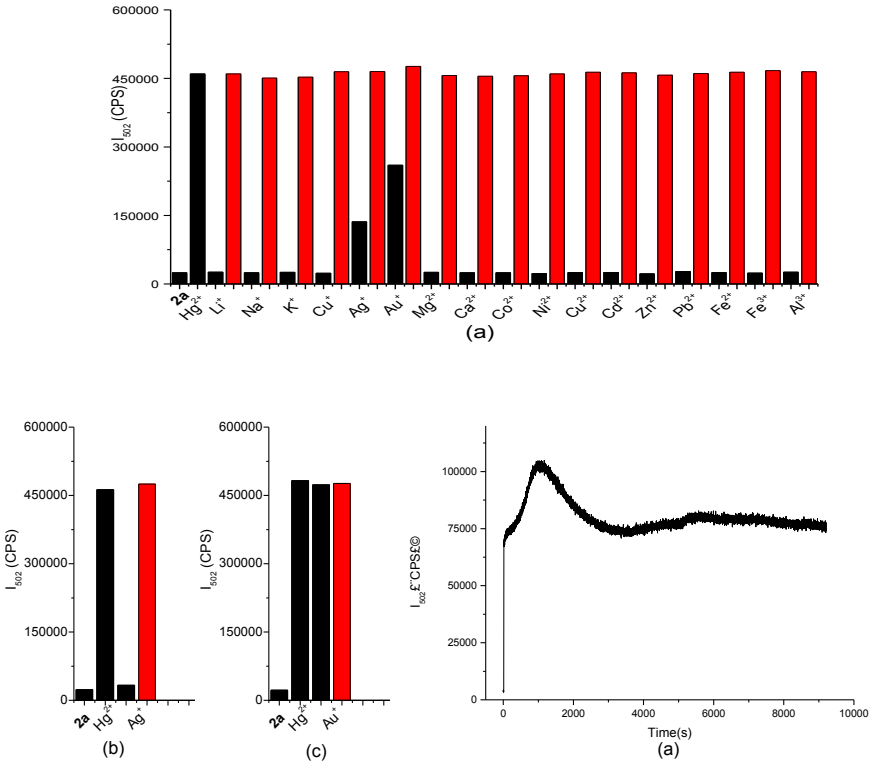

Figure S13. a-c) Emission intensity of probe **2a** (2 μM) upon the addition of different competing metal ions (50 equiv., each) and Hg^{2+} (5 equiv.). Black bars: free probe **2a**, or treated with the marked metal ions (50 equiv.); red bars: the probe treated with the marked metal ions (50 equiv.) followed by Hg^{2+} (5 equiv.). (All fluorescence responses were obtained after 15 min incubation time in 20 mM PBS buffer containing 0.2 % DMSO at 25 °C with λ_{ex} = 477 nm and λ_{em} = 502 nm unless otherwise stated; 20 mM PBS buffered normal saline containing 0.2 % DMSO and 154 mM NaCl was used in b); incubation time was 2h for c); d) The fluorescence intensity of probe **2a** (2 μM) incubated with Au^{+} (100 equiv.) in 0.02 M PBS buffer containing 0.2% DMSO at 502 nm for 0-150 min (excited at 477 nm, 2 nm slit width for both excitation and emission).

Cell culture:

MCF-7 cells were purchased from the American Type Culture Collection (ATCC). The cells were cultured in Dulbecco's Modified Eagle Medium (DMEM) supplemented with 10% fetal bovine serum (FBS), maintained at 37 °C in a humidified atmosphere containing 95% air and 5% CO_2.

Cytotoxicity assay:

Cell survival was evaluated by the MTS assay (CellTiter 96 AQueous One Solution Reagent), based on the conversion of a tetrazolium compound, 3-(4,5-dimethylthiazol-2-yl)-5-(3-carboxymethoxy-phenyl)-2-(4-sulfophenyl)-2H tetrazolium (MTS), to a colored formazan product by living cells.[4] Absorbance was

read by a microplate reader (Molecular Devices SpectraMax I3) at 490 nm. The quantity of formazan product, as measured by the amount of absorbance, was directly proportional to the metabolic activity of viable cells in the culture.
Cell viability (% of control) = $(OD_{EG}-OD_{ZG})/(OD_{CG}-OD_{ZG})*100\%$
IC_{50} value was calculated using GraphPad Prism software based on the cell viability data at different concentrations.

Determination of Hg^{2+} concentration in *in vitro* imaging experiments:
Cytotoxcicity assay was performed according the protocol above. Hg^{2+} concentration of 10 μM with cell viability 65.13±4.11% was used in *in vitro* fluorescent imaging experiment.

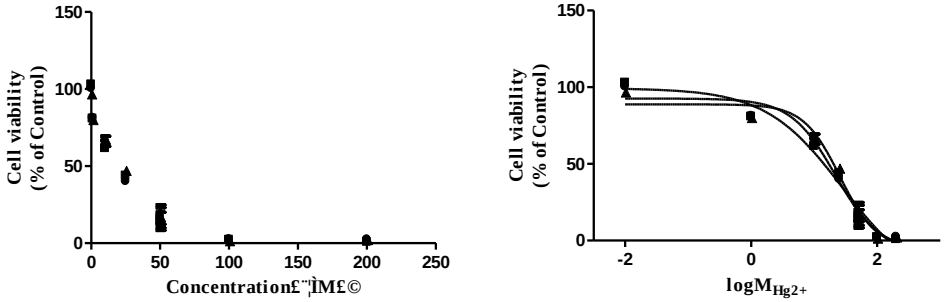

Figure S14. Cytotoxicity of Hg^{2+} at various concentrations for MCF-7 cells after 24 h incubation (IC_{50} = 25.01±3.16 μM).

Cytotoxicity of the probes (1a, 2a, and 4) and determination of probe concentration (1a, 2a) in *in vitro* imaging experiments:
Cytotoxcicity assays were performed according the protocol above. The IC_{50} value of the probe **2a** was determined as 214.13±6.14 μM. The IC_{50} value of the probe **4** was determined as 28.44±2.05 μM. Probe **1a** showed no significant toxicity up to 250 μM. 20.0 μM concentration of **1a** and **2a** was selected in *in vitro* imaging experiment.

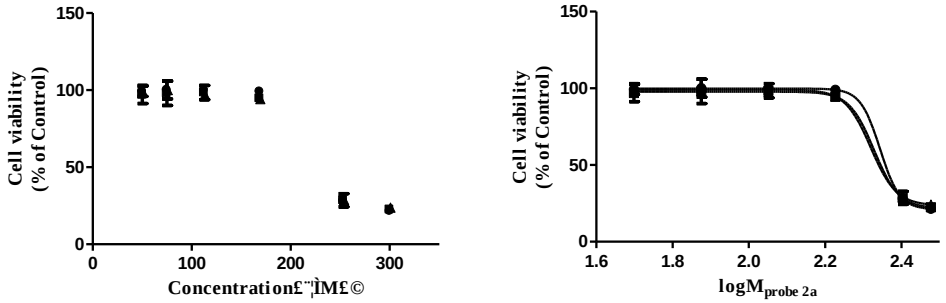

Figure S15. Cytotoxicity of the probe **2a** at various concentrations for MCF-7 cells after 24 h incubation (IC_{50} = 214.13±6.14 μM).

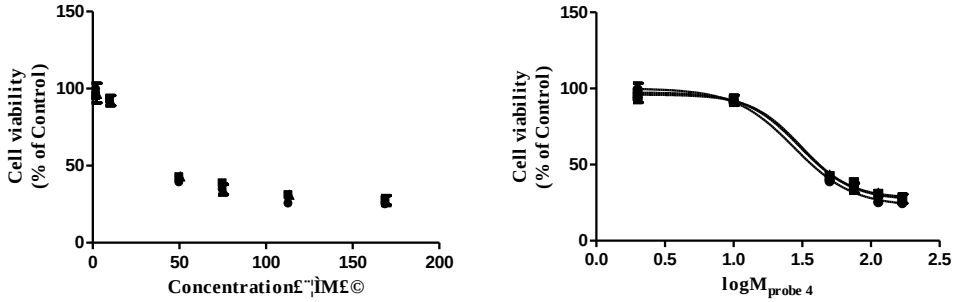

Figure S16. Cytotoxicity of the probe **4** at various concentrations for MCF-7 cells after 24 h incubation (IC_{50} = 28.44±2.05 μM).

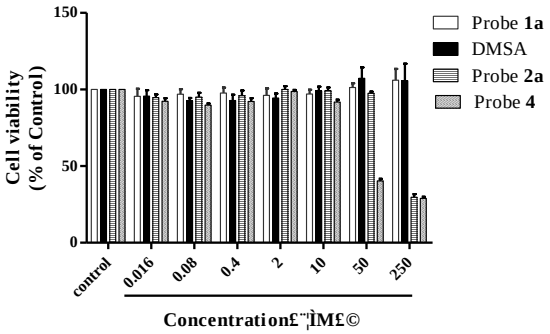

Figure S17. Cell viabilities of probe **1a**, DMSA, probe **2a**, and probe **4** at various concentrations for MCF-7 cells after 24 h incubation.

***In vitro* fluorescent imaging of Hg^{2+} in MCF-7 cells:**

MCF-7 cells were seeded at 5 × 10^4 per well in a 24-well culture plate with flat glass bottom and grown in Dulbecco's Modified Eagle Medium (DMEM) with 10% fetal bovine serum and 1% glutamate in a 5% CO_2 incubator at 37 ^oC. After 12 h, cell culture media was removed from wells and cells in each well were washed with D-Hanks for three times. The washed cells were incubated in either 10 μM Hg^{2+} DMEM solution without serum for 1h or DMEM without serum (control). DMEM solution without Hg^{2+} was removed from wells and cells in each well were washed with D-Hanks for three times. The cells were then treated with 20 μM probe (**1a** or **2a**) DMEM solution for a specific time (30 min or 4 h). DMEM solution containing Hg^{2+} was removed from wells and cells in each well were washed with D-Hanks for three times. The cells were then treated with 20 μM probe (**1a** or **2a**) DMEM solution for a specific time (30 min or 4 h). After removal of the probe DMEM solution, cells in each well were washed with D-Hanks for three times and DMEM without phenol red was added. The culture plate was then imaged with Nikon A1R Confocal Microscope (excited at 488 nm, emission collected from 514 to 554 nm).

Evaluation of protective effects of probes (1a, 2a, and 4) against the Hg^{2+}-induced cytotoxicity through cell viability assays

MCF-7 cells were seeded into 96 wells plates at a density of 1×10^5 per mL and grown in DMEM with 10% fetal bovine serum and 1% glutamate. After 12 h, cell culture media were removed from wells and cells in each well were washed with D-Hanks for 3 times before experiments. A solution of 10 μM Hg^{2+} in serum free DMEM was prepared by dilution of a stock solution of $Hg(ClO_4)_4$ (10 mM) in DMSO. Fresh stock solutions of 10 mM of each probe were prepared by first dissolving the probe in small amount of dimethyl sulfoxide (DMSO) and then diluted by serum-free DMEM before experiments. A series of different concentrations (0.5, 1.0, 5.0, 25, 50, 100 μM) of each probe in serum-free DMEM were prepared by dilution of the corresponding stock solution for experimental I. A series of different concentrations (0.05, 0.1, 0.5, 2.5, 5.0, 10 μM) of each probe in serum-free DMEM were prepared by dilution of the corresponding stock solution for experimental II and III. The wells in the plate were divided into 4 groups: the zero group, the control (DMSA) group, the Hg^{2+} group, and the Hg^{2+} plus probe group.

Experiment I: 100 μL of 10 μM Hg^{2+} in serum free DMEM was added to wells of the Hg^{2+} group and the Hg^{2+} plus probe group. Equal volume of serum-free DMEM was added to wells of the zero and the control group. After 2 h, 11.0 μL of different concentrations (0.5, 1.0, 5.0, 25, 50, 100 μM) of each probe in serum free fresh medium were added to wells of the Hg^{2+} plus probe group to the required final concentration (0.05, 0.1, 0.5, 2.5, 5.0, 10 μM). Equal volumes of serum-free DMEM were added to the zero group, the control group, and the Hg^{2+} group. After 24 h, MTS (20 μL $well^{-1}$) was added to each well. And 3 h later, the MTS formazan product in each well was measured by determining the absorbance at 490 nm. The data were expressed as the number of percentage of the control value and mean ± SEM (standard error of measurement) of three independent experiments. (Results was shown in Fig. 5)

Experiment II: 100 μL of 10 μM Hg^{2+} in serum free DMEM was added to wells of the Hg^{2+} group and the Hg^{2+} plus probe group. Equal volume of serum-free DMEM was added to wells of the zero and the control group. After 24 h, the medium was discarded and then washed three times by D-Hanks. 100 μL of different concentrations (0.05, 0.1, 0.5, 2.5, 5.0, 10 μM) of each probe in serum free fresh medium were added to the wells of the Hg^{2+} plus probe group. Equal volumes of serum-free DMEM were added to the zero group, the control group, and the Hg^{2+} group. After 24 h, MTS (20 μl $well^{-1}$) was added to each well. And 3 h later, the MTS formazan product in each well was measured by determining the absorbance at 490 nm. The data were expressed as the number of percentage of the control value and mean ± SEM of three independent experiments.

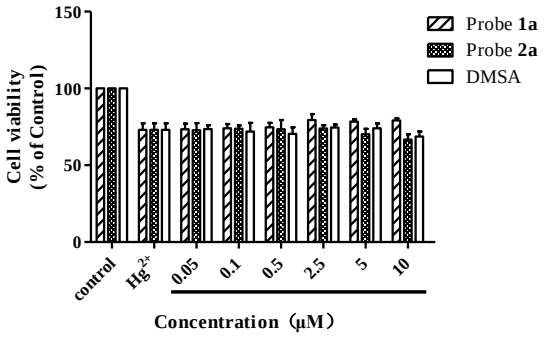

Figure S18. Cell viability (24 h) of probe **1**, **2**, and DMSA at various concentrations for MCF-7 cells pretreated with10 μM Hg^{2+} for 24 h.

Experiment III: 100 μL of different concentrations (0.05, 0.1, 0.5, 2.5, 5.0, 10 μM) of each probe in serum free fresh medium were added to wells of the Hg^{2+} plus probe group. Equal volume of serum-free DMEM was added to wells of the zero group, the control group, and the Hg^{2+} group. After 24 h, the medium was discarded and then washed three times by D-Hanks. 100 μL of 10 μM Hg^{2+} in serum free DMEM was added to wells of the Hg^{2+} group and the Hg^{2+} plus probe group. Equal volume of serum-free DMEM was added to wells of the zero group and the control group. After 24 h, MTS (20 μl per well) was added to each well. And 3 h later, the MTS formazan product in each well was measured by determining the absorbance at 490 nm. The data were expressed as the number of percentage of the control value and mean ± SEM (standard error of measurement) of three independent experiments.

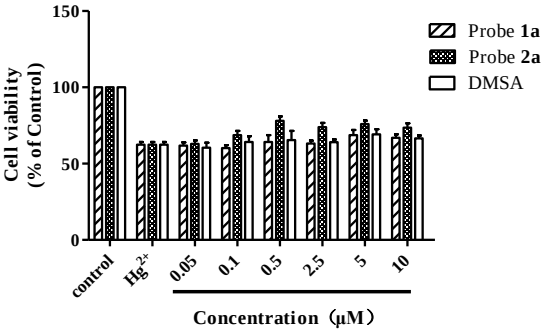

Figure S19. Cell viability (24 h) of10 μM Hg^{2+} pretreated with probe **1a, 2a** and DMSA at various concentrations for MCF-7 cells for 24 h.

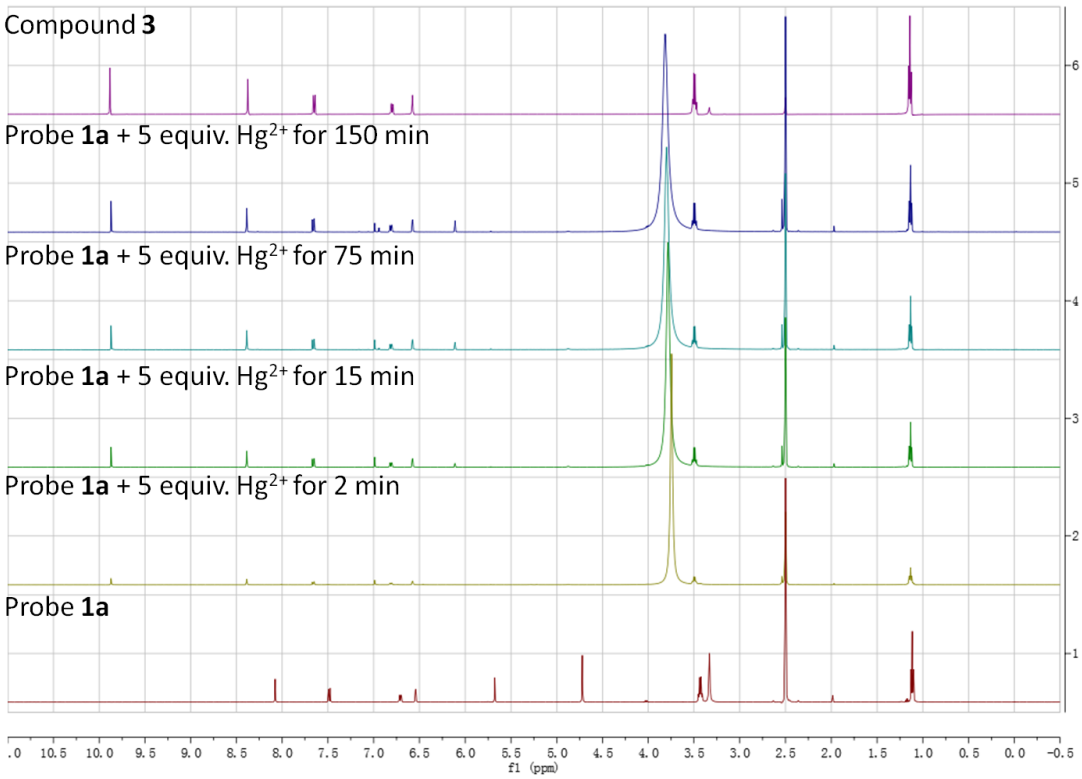

Figure S20. ^{1}H NMR (500 MHz, DMSO-d_6) of probe **1a,** probe **1a** with 5 equiv. Hg^{2+} in different time points (2, 15 and 150 min) and the compound **3. (**Clearly, the aldehyde **3** was formed as a product.)

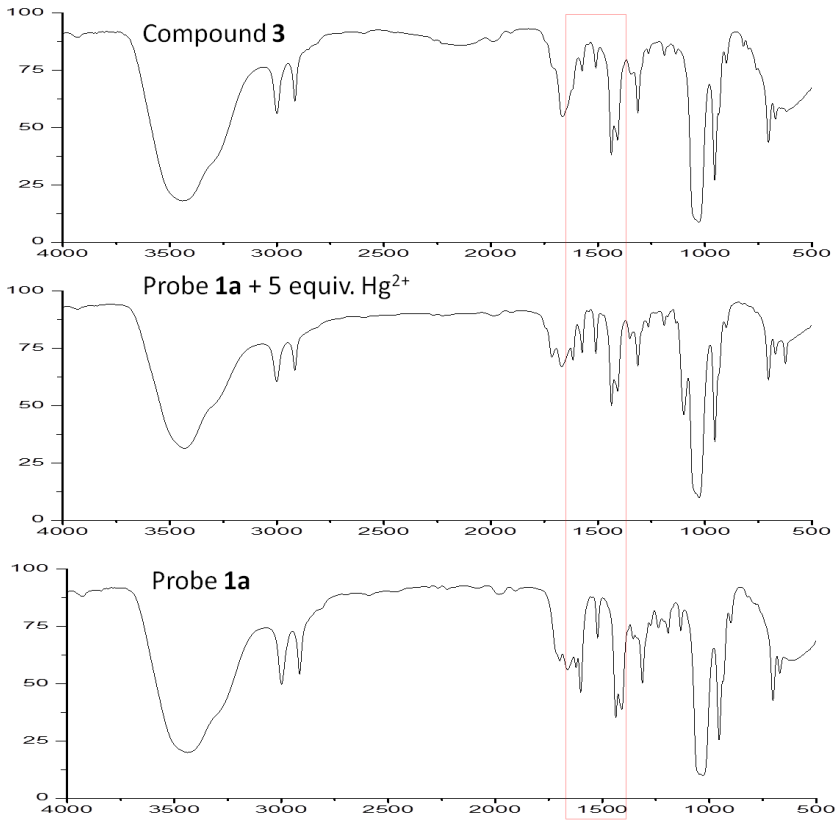

Figure S21. IR spectrum of probe **1a**, probe **1a** with 5 equiv. Hg^{2+} for 12 h and the compound **3**. (The highlighted IR region supported formation of the compound **3**)

NMR spectra of compound **1a**

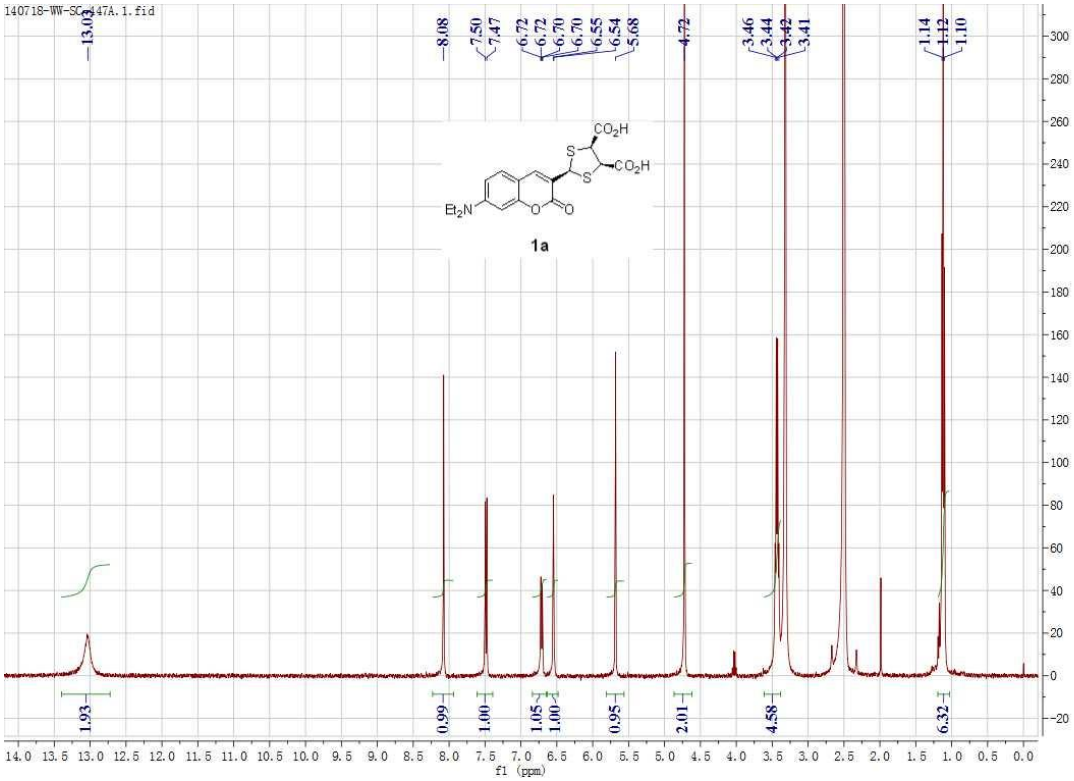

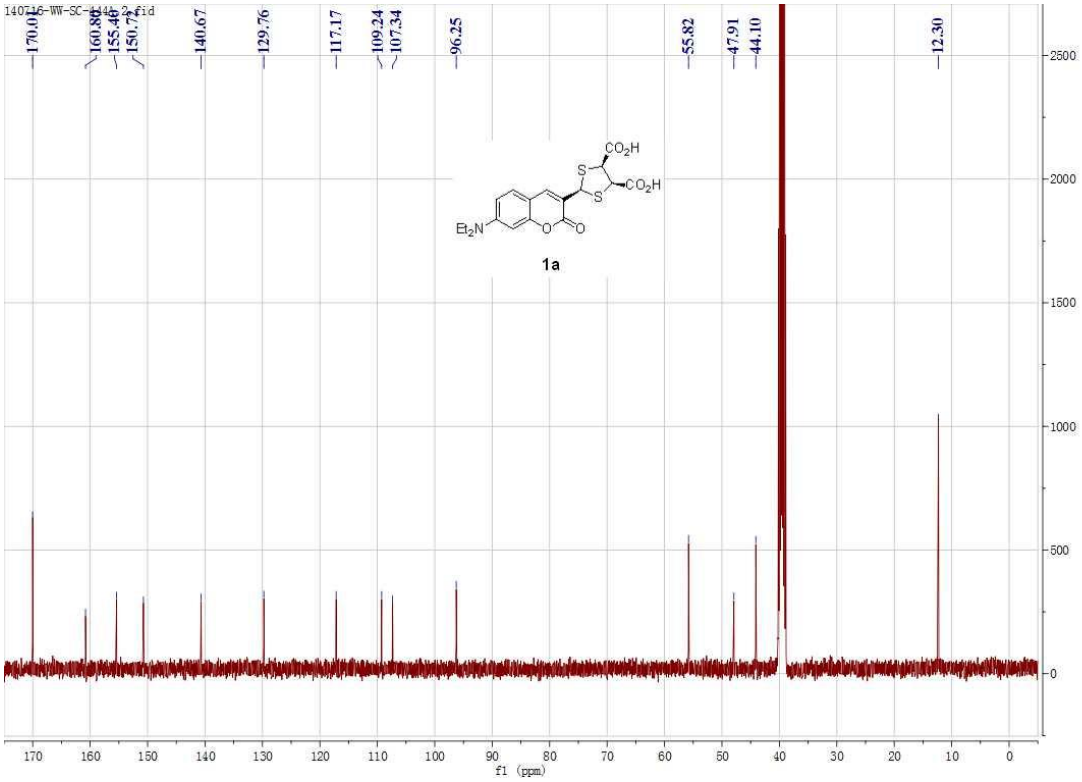

2D-NOESY spectum of compound **1a**

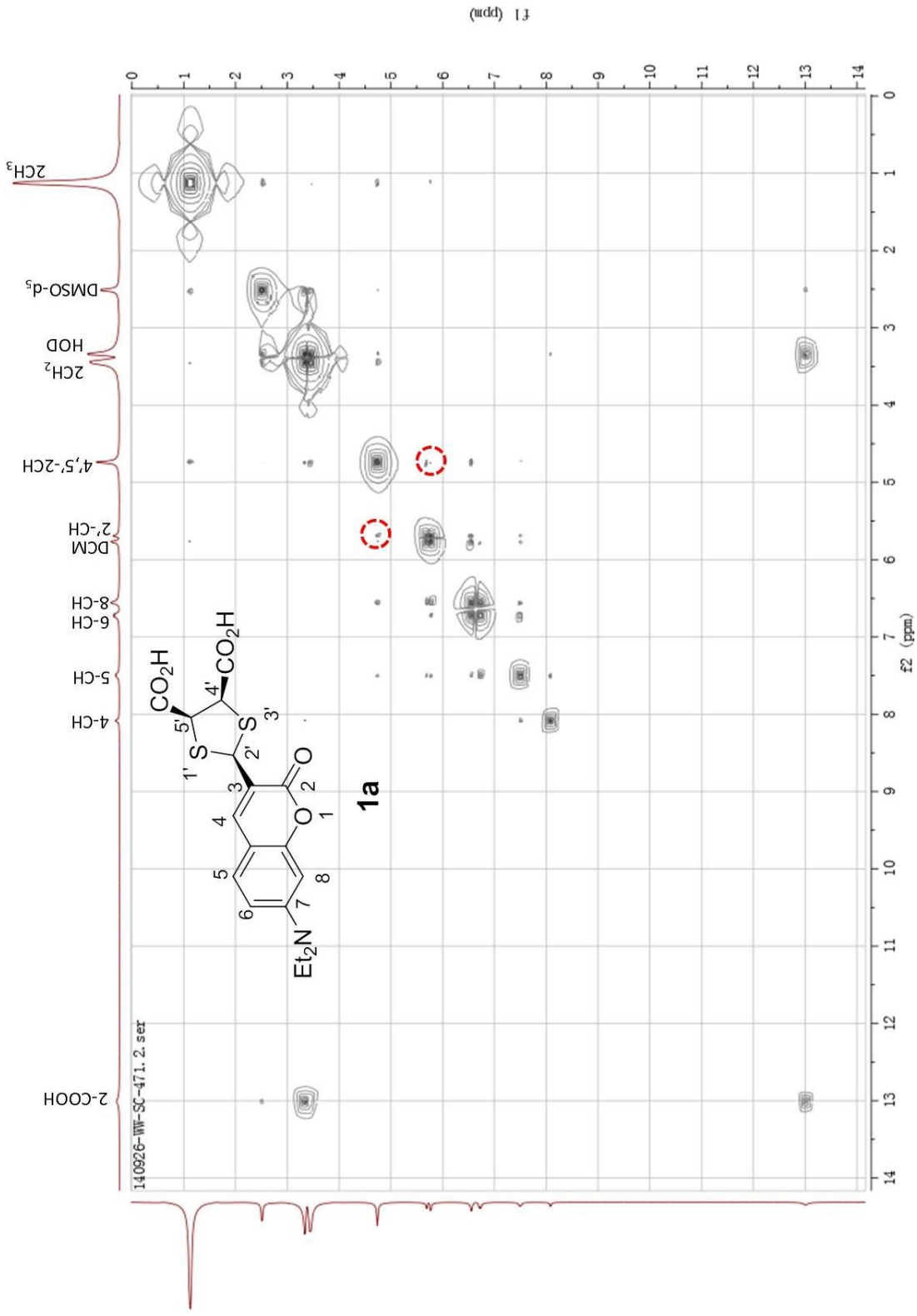

NMR spectra of compound **1b**

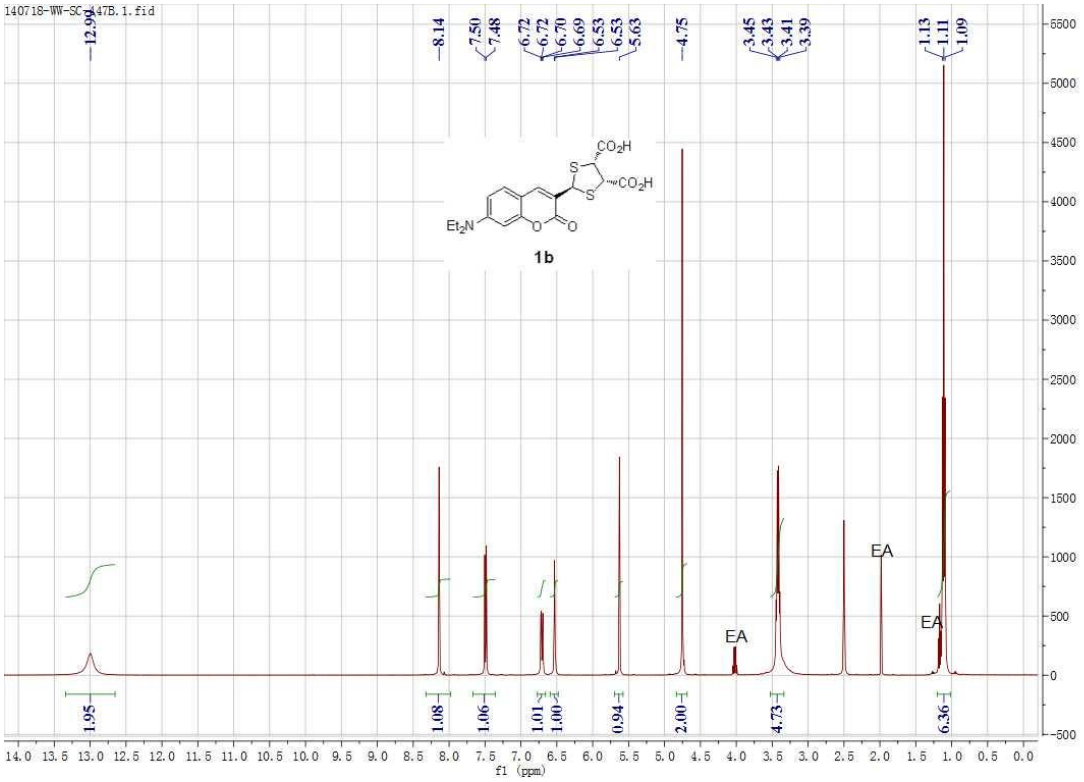

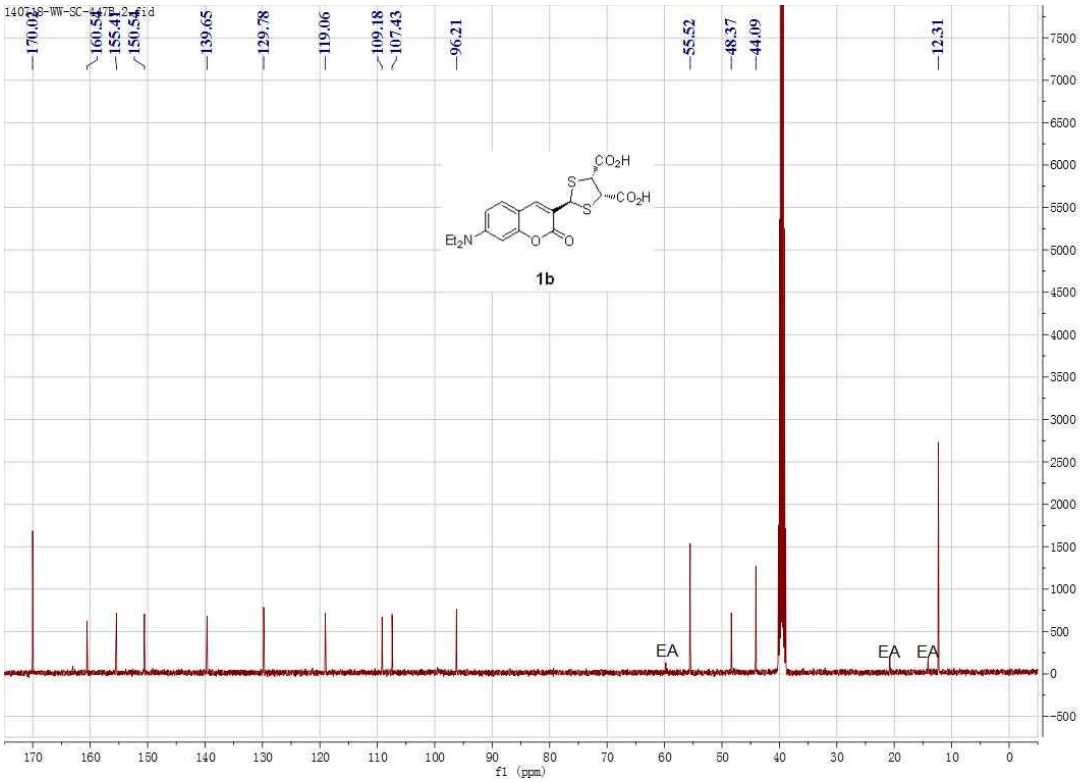

NMR spectra of compound **2a**

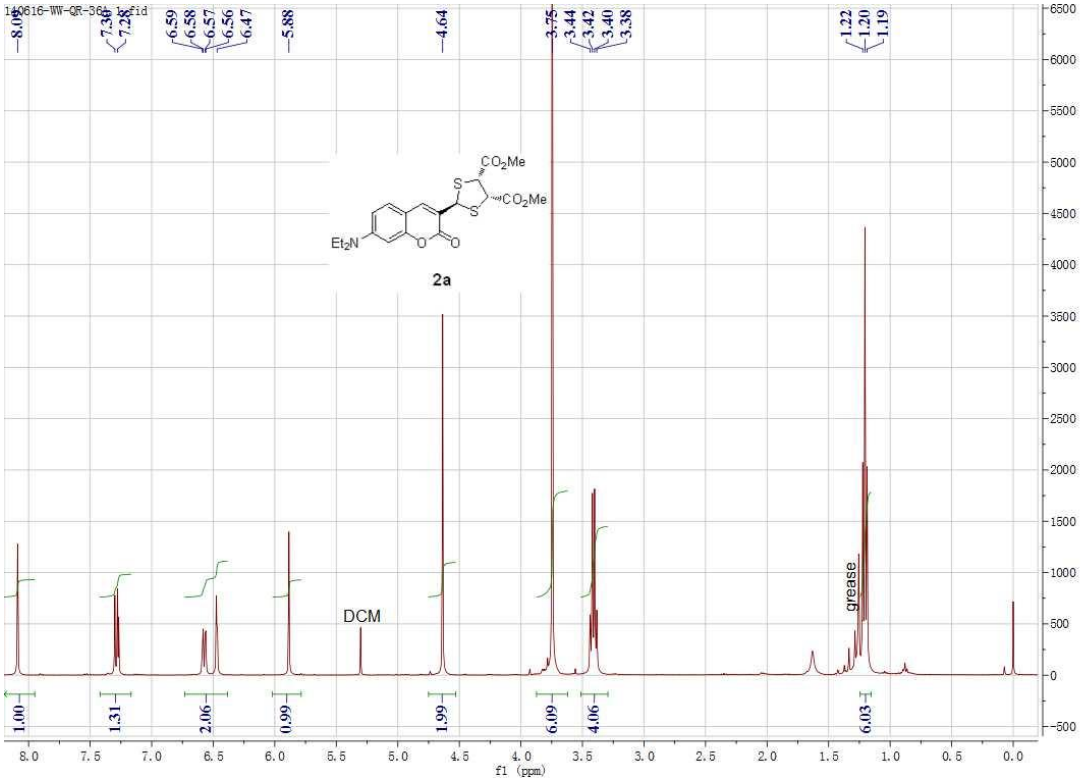

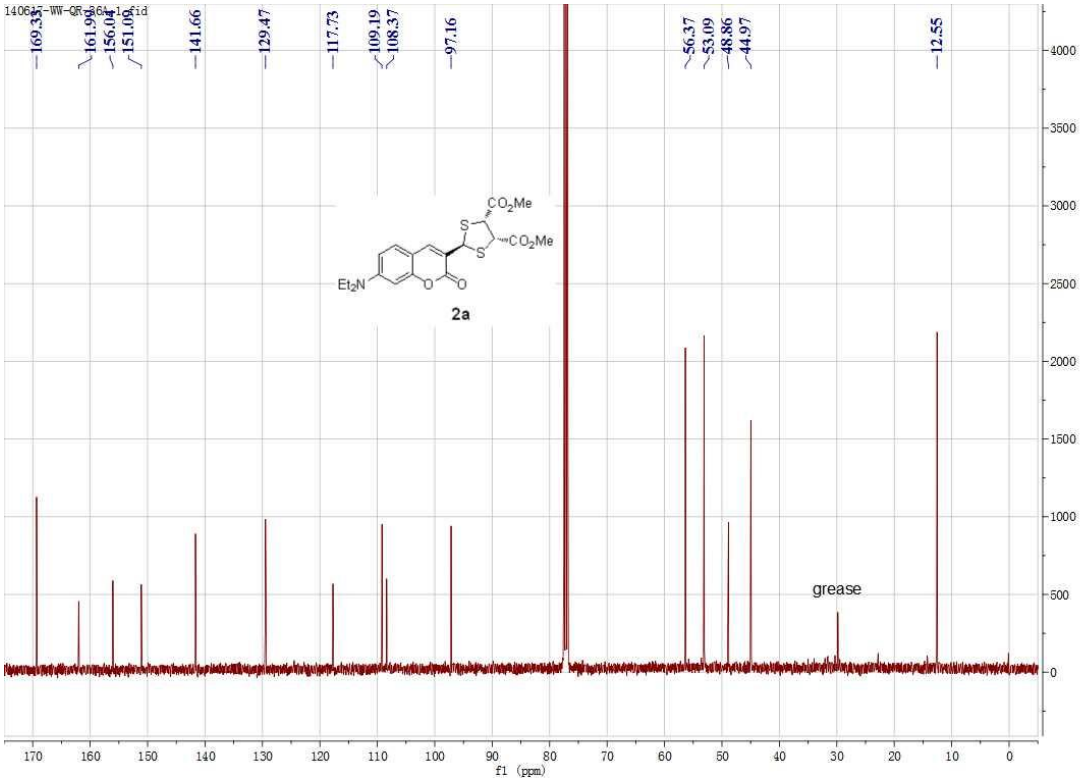

2D-NOESY spectrum of compound **2a**

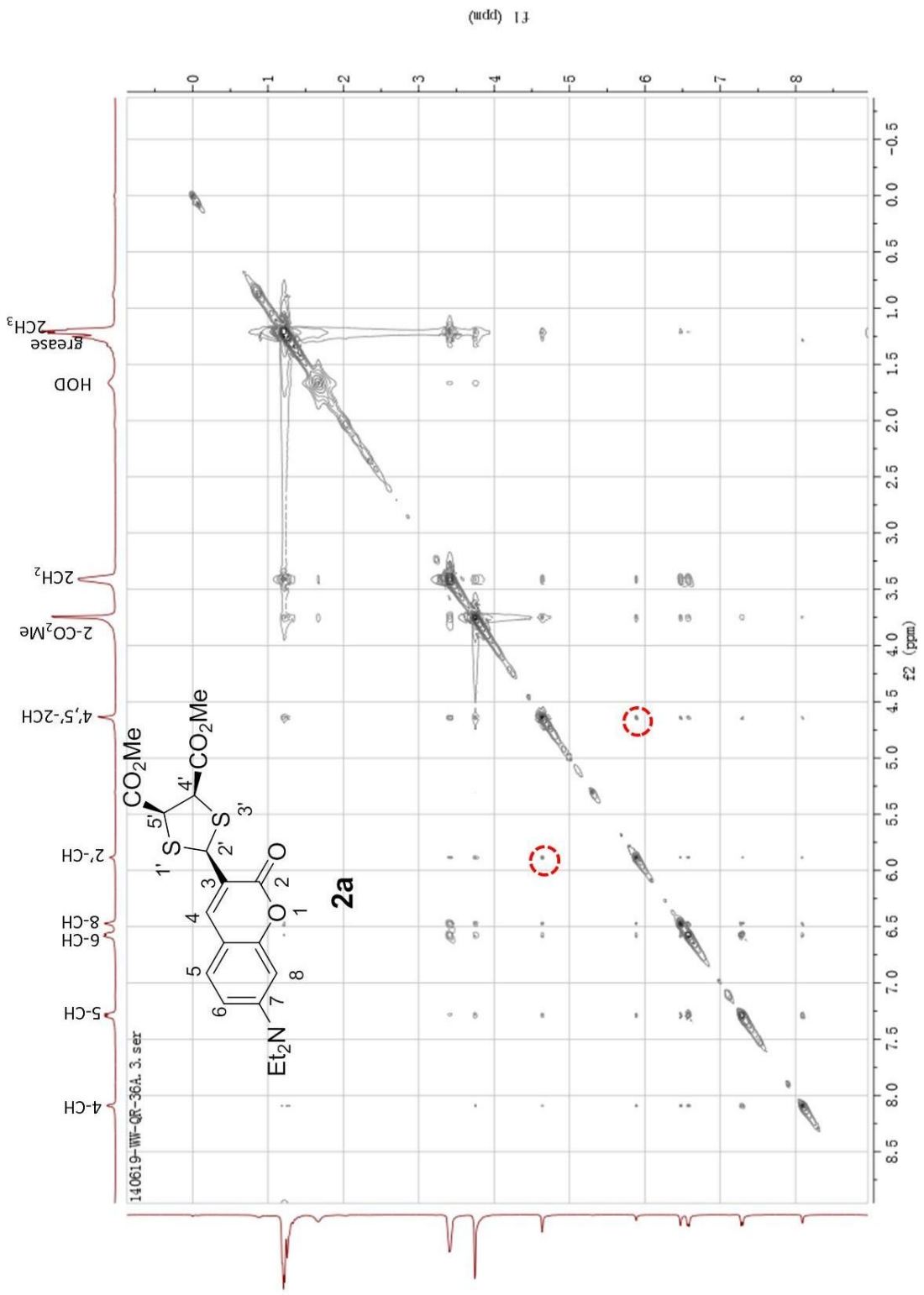

Crystal Structure and Data for probe **2a**

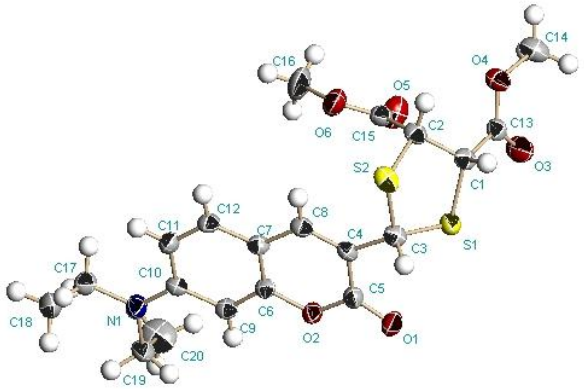

Figure S22. Crystallographic representation of probe **2a**.

Table S1. Crystal data and structure refinement for cd214397.

Identification code	cd214397	
Empirical formula	C20 H23 N O6 S2	
Formula weight	437.51	
Temperature	293(2) K	
Wavelength	0.71073 Å	
Crystal system	Monoclinic	
Space group	P 21	
Unit cell dimensions	a = 9.1418(9) Å	α= 90°.
	b = 9.3880(10) Å	β= 110.690(2)°.
	c = 12.6939(13) Å	γ = 90°.
Volume	1019.17(18) $Å^3$	
Z	2	
Density (calculated)	1.426 Mg/m^3	
Absorption coefficient	0.299 mm^{-1}	
F(000)	460	
Crystal size	0.176 x 0.143 x 0.112 mm^3	
Theta range for data collection	1.715 to 25.996°.	
Index ranges	-9<=h<=11, -11<=k<=11, -15<=l<=15	
Reflections collected	6226	
Independent reflections	3694 [R(int) = 0.0273]	
Completeness to theta = 25.242°	99.8 %	
Absorption correction	Semi-empirical from equivalents	
Max. and min. transmission	0.7457 and 0.6412	

Refinement method	Full-matrix least-squares on F^2
Data / restraints / parameters	3694 / 1 / 266
Goodness-of-fit on F^2	1.025
Final R indices [I>2sigma(I)]	R1 = 0.0403, wR2 = 0.0941
R indices (all data)	R1 = 0.0459, wR2 = 0.0974
Absolute structure parameter	0.09(6)
Extinction coefficient	n/a
Largest diff. peak and hole	0.259 and -0.173 e.$Å^{-3}$

Table S2. Atomic coordinates (x 10^4) and equivalent isotropic displacement parameters ($Å^2$x 10^3) for cd214397. U(eq) is defined as one third of the trace of the orthogonalized U^{ij} tensor.

	x	y	z	U(eq)
S(1)	10943(1)	6325(1)	7367(1)	41(1)
S(2)	8227(1)	8251(1)	6994(1)	42(1)
N(1)	4202(4)	581(3)	8710(3)	39(1)
O(1)	10832(3)	4643(3)	9375(2)	47(1)
O(2)	8697(3)	3367(3)	9048(2)	34(1)
O(3)	12048(3)	6112(4)	5439(2)	58(1)
O(4)	10295(3)	7603(3)	4293(2)	44(1)
O(5)	8199(3)	5461(3)	4791(3)	57(1)
O(6)	6157(3)	6554(4)	4991(2)	54(1)
C(1)	10346(4)	7475(4)	6130(3)	36(1)
C(2)	8591(4)	7710(4)	5743(3)	37(1)
C(3)	9414(4)	6897(4)	7922(3)	36(1)
C(4)	8503(4)	5629(4)	8093(3)	31(1)
C(5)	9442(4)	4569(4)	8869(3)	33(1)
C(6)	7099(4)	3191(4)	8578(3)	30(1)
C(7)	6186(4)	4238(4)	7861(3)	32(1)
C(8)	6949(4)	5457(4)	7629(3)	33(1)
C(9)	6493(4)	1975(4)	8854(3)	34(1)
C(10)	4853(4)	1761(4)	8431(3)	32(1)
C(11)	3923(4)	2830(4)	7728(3)	37(1)
C(12)	4563(4)	4008(4)	7448(3)	37(1)
C(13)	10992(4)	6936(4)	5263(3)	36(1)
C(14)	11005(6)	7415(5)	3463(3)	55(1)
C(15)	7655(4)	6436(4)	5137(3)	36(1)
C(16)	5155(5)	5413(7)	4397(4)	72(2)
C(17)	2525(4)	301(4)	8263(3)	42(1)
C(18)	1689(5)	884(6)	8994(4)	56(1)
C(19)	5138(5)	-533(5)	9437(3)	43(1)
C(20)	5603(7)	-1662(6)	8789(4)	79(2)

Table 3. Bond lengths [Å] and angles [°] for cd214397.

S(1)-C(1)	1.823(4)
S(1)-C(3)	1.853(4)
S(2)-C(2)	1.806(4)
S(2)-C(3)	1.811(4)
N(1)-C(10)	1.363(5)
N(1)-C(19)	1.456(5)
N(1)-C(17)	1.459(5)
O(1)-C(5)	1.206(4)
O(2)-C(5)	1.378(4)
O(2)-C(6)	1.378(4)
O(3)-C(13)	1.195(5)
O(4)-C(13)	1.327(4)
O(4)-C(14)	1.430(5)
O(5)-C(15)	1.196(5)
O(6)-C(15)	1.320(4)
O(6)-C(16)	1.438(6)
C(1)-C(13)	1.508(5)
C(1)-C(2)	1.518(5)
C(1)-H(1)	0.9800
C(2)-C(15)	1.513(5)
C(2)-H(2)	0.9800
C(3)-C(4)	1.512(5)
C(3)-H(3)	0.9800
C(4)-C(8)	1.342(5)
C(4)-C(5)	1.449(5)
C(6)-C(9)	1.368(5)
C(6)-C(7)	1.398(5)
C(7)-C(12)	1.405(5)
C(7)-C(8)	1.424(5)
C(8)-H(8)	0.9300
C(9)-C(10)	1.417(5)
C(9)-H(9)	0.9300
C(10)-C(11)	1.411(5)
C(11)-C(12)	1.356(5)
C(11)-H(11)	0.9300
C(12)-H(12)	0.9300
C(14)-H(14A)	0.9600

C(14)-H(14B)	0.9600
C(14)-H(14C)	0.9600
C(16)-H(16A)	0.9600
C(16)-H(16B)	0.9600
C(16)-H(16C)	0.9600
C(17)-C(18)	1.499(6)
C(17)-H(17A)	0.9700
C(17)-H(17B)	0.9700
C(18)-H(18A)	0.9600
C(18)-H(18B)	0.9600
C(18)-H(18C)	0.9600
C(19)-C(20)	1.493(7)
C(19)-H(19A)	0.9700
C(19)-H(19B)	0.9700
C(20)-H(20A)	0.9600
C(20)-H(20B)	0.9600
C(20)-H(20C)	0.9600

C(1)-S(1)-C(3)	96.83(17)
C(2)-S(2)-C(3)	96.89(17)
C(10)-N(1)-C(19)	122.4(3)
C(10)-N(1)-C(17)	122.8(3)
C(19)-N(1)-C(17)	114.7(3)
C(5)-O(2)-C(6)	122.5(3)
C(13)-O(4)-C(14)	115.6(3)
C(15)-O(6)-C(16)	116.7(4)
C(13)-C(1)-C(2)	117.0(3)
C(13)-C(1)-S(1)	110.7(3)
C(2)-C(1)-S(1)	109.0(2)
C(13)-C(1)-H(1)	106.5
C(2)-C(1)-H(1)	106.5
S(1)-C(1)-H(1)	106.5
C(15)-C(2)-C(1)	113.1(3)
C(15)-C(2)-S(2)	115.0(3)
C(1)-C(2)-S(2)	105.0(2)
C(15)-C(2)-H(2)	107.8
C(1)-C(2)-H(2)	107.8
S(2)-C(2)-H(2)	107.8

C(4)-C(3)-S(2)	114.4(2)
C(4)-C(3)-S(1)	110.8(3)
S(2)-C(3)-S(1)	108.39(18)
C(4)-C(3)-H(3)	107.7
S(2)-C(3)-H(3)	107.7
S(1)-C(3)-H(3)	107.7
C(8)-C(4)-C(5)	119.8(3)
C(8)-C(4)-C(3)	125.7(3)
C(5)-C(4)-C(3)	114.5(3)
O(1)-C(5)-O(2)	116.7(3)
O(1)-C(5)-C(4)	125.6(3)
O(2)-C(5)-C(4)	117.8(3)
C(9)-C(6)-O(2)	116.9(3)
C(9)-C(6)-C(7)	123.4(3)
O(2)-C(6)-C(7)	119.7(3)
C(6)-C(7)-C(12)	116.4(3)
C(6)-C(7)-C(8)	118.5(3)
C(12)-C(7)-C(8)	125.2(3)
C(4)-C(8)-C(7)	121.7(3)
C(4)-C(8)-H(8)	119.1
C(7)-C(8)-H(8)	119.1
C(6)-C(9)-C(10)	119.4(3)
C(6)-C(9)-H(9)	120.3
C(10)-C(9)-H(9)	120.3
N(1)-C(10)-C(11)	121.4(3)
N(1)-C(10)-C(9)	121.1(3)
C(11)-C(10)-C(9)	117.4(3)
C(12)-C(11)-C(10)	121.7(3)
C(12)-C(11)-H(11)	119.1
C(10)-C(11)-H(11)	119.1
C(11)-C(12)-C(7)	121.6(3)
C(11)-C(12)-H(12)	119.2
C(7)-C(12)-H(12)	119.2
O(3)-C(13)-O(4)	124.8(4)
O(3)-C(13)-C(1)	125.4(3)
O(4)-C(13)-C(1)	109.6(3)
O(4)-C(14)-H(14A)	109.5
O(4)-C(14)-H(14B)	109.5

H(14A)-C(14)-H(14B)	109.5
O(4)-C(14)-H(14C)	109.5
H(14A)-C(14)-H(14C)	109.5
H(14B)-C(14)-H(14C)	109.5
O(5)-C(15)-O(6)	123.9(4)
O(5)-C(15)-C(2)	123.9(3)
O(6)-C(15)-C(2)	112.2(3)
O(6)-C(16)-H(16A)	109.5
O(6)-C(16)-H(16B)	109.5
H(16A)-C(16)-H(16B)	109.5
O(6)-C(16)-H(16C)	109.5
H(16A)-C(16)-H(16C)	109.5
H(16B)-C(16)-H(16C)	109.5
N(1)-C(17)-C(18)	112.9(3)
N(1)-C(17)-H(17A)	109.0
C(18)-C(17)-H(17A)	109.0
N(1)-C(17)-H(17B)	109.0
C(18)-C(17)-H(17B)	109.0
H(17A)-C(17)-H(17B)	107.8
C(17)-C(18)-H(18A)	109.5
C(17)-C(18)-H(18B)	109.5
H(18A)-C(18)-H(18B)	109.5
C(17)-C(18)-H(18C)	109.5
H(18A)-C(18)-H(18C)	109.5
H(18B)-C(18)-H(18C)	109.5
N(1)-C(19)-C(20)	112.3(3)
N(1)-C(19)-H(19A)	109.1
C(20)-C(19)-H(19A)	109.1
N(1)-C(19)-H(19B)	109.1
C(20)-C(19)-H(19B)	109.1
H(19A)-C(19)-H(19B)	107.9
C(19)-C(20)-H(20A)	109.5
C(19)-C(20)-H(20B)	109.5
H(20A)-C(20)-H(20B)	109.5
C(19)-C(20)-H(20C)	109.5
H(20A)-C(20)-H(20C)	109.5
H(20B)-C(20)-H(20C)	109.5

Symmetry transformations used to generate equivalent atoms:

Table S4. Anisotropic displacement parameters ($Å^2$ x 10^3) for cd214397. The anisotropic displacement factor exponent takes the form: $-2\pi^2[h^2 a^{*2}U^{11} + .+ 2 h k a^* b^* U^{12}]$

	U^{11}	U^{22}	U^{33}	U^{23}	U^{13}	U^{12}
S(1)	36(1)	46(1)	41(1)	9(1)	15(1)	0(1)
S(2)	56(1)	27(1)	51(1)	2(1)	28(1)	4(1)
N(1)	35(2)	36(2)	46(2)	7(2)	13(1)	-3(2)
O(1)	32(1)	49(2)	53(2)	6(1)	7(1)	-7(1)
O(2)	28(1)	31(1)	41(1)	7(1)	10(1)	3(1)
O(3)	53(2)	70(2)	57(2)	16(2)	26(1)	21(2)
O(4)	52(2)	41(2)	41(1)	9(1)	21(1)	6(1)
O(5)	50(2)	42(2)	76(2)	-16(2)	20(2)	-4(2)
O(6)	37(1)	70(2)	53(2)	-7(2)	13(1)	-4(2)
C(1)	41(2)	30(2)	35(2)	0(2)	13(2)	-9(2)
C(2)	43(2)	30(2)	39(2)	7(2)	17(2)	3(2)
C(3)	43(2)	30(2)	33(2)	-2(2)	13(2)	-4(2)
C(4)	38(2)	28(2)	28(2)	-1(2)	15(2)	-1(2)
C(5)	34(2)	34(2)	34(2)	-3(2)	14(2)	-2(2)
C(6)	28(2)	30(2)	32(2)	1(2)	12(1)	4(2)
C(7)	36(2)	28(2)	31(2)	3(2)	11(1)	4(2)
C(8)	40(2)	30(2)	31(2)	4(2)	13(2)	5(2)
C(9)	36(2)	30(2)	35(2)	5(2)	12(2)	7(2)
C(10)	37(2)	31(2)	28(2)	1(1)	13(2)	1(2)
C(11)	28(2)	40(2)	39(2)	2(2)	9(2)	-2(2)
C(12)	36(2)	35(2)	35(2)	9(2)	8(2)	5(2)
C(13)	34(2)	34(2)	39(2)	2(2)	13(2)	-6(2)
C(14)	73(3)	54(3)	44(2)	5(2)	28(2)	0(3)
C(15)	40(2)	36(2)	34(2)	4(2)	12(2)	1(2)
C(16)	41(2)	99(4)	71(3)	-16(3)	13(2)	-25(3)
C(17)	42(2)	38(2)	41(2)	0(2)	10(2)	-9(2)
C(18)	43(2)	78(4)	51(2)	9(2)	21(2)	-2(2)
C(19)	43(2)	41(2)	44(2)	12(2)	16(2)	-1(2)
C(20)	95(4)	56(3)	90(4)	6(3)	35(3)	29(3)

Table 5. Hydrogen coordinates (× 10^4) and isotropic displacement parameters (Å^2 × 10^3) for cd214397.

	x	y	z	U (eq)
H(1)	10835	8404	6380	43
H(2)	8332	8515	5218	44
H(3)	9940	7338	8659	43
H(8)	6354	6152	7143	40
H(9)	7152	1294	9316	41
H(11)	2842	2724	7449	44
H(12)	3911	4681	6972	44
H(14A)	12055	7775	3748	83
H(14B)	10414	7925	2792	83
H(14C)	11022	6421	3293	83
H(16A)	5171	5353	3646	109
H(16B)	4106	5592	4365	109
H(16C)	5519	4531	4784	109
H(17A)	2355	-720	8186	50
H(17B)	2081	720	7519	50
H(18A)	2166	521	9745	84
H(18B)	611	600	8698	84
H(18C)	1755	1905	9008	84
H(19A)	4544	-963	9853	51
H(19B)	6071	-112	9976	51
H(20A)	4697	-1985	8182	119
H(20B)	6063	-2447	9279	119
H(20C)	6350	-1280	8490	119

Table 6. Torsion angles [°] for cd214397.

C(3)-S(1)-C(1)-C(13)	-160.4(2)
C(3)-S(1)-C(1)-C(2)	-30.3(3)
C(13)-C(1)-C(2)-C(15)	50.8(4)
S(1)-C(1)-C(2)-C(15)	-75.7(3)
C(13)-C(1)-C(2)-S(2)	176.9(3)
S(1)-C(1)-C(2)-S(2)	50.4(3)
C(3)-S(2)-C(2)-C(15)	78.9(3)
C(3)-S(2)-C(2)-C(1)	-46.1(3)
C(2)-S(2)-C(3)-C(4)	-98.8(3)
C(2)-S(2)-C(3)-S(1)	25.3(2)
C(1)-S(1)-C(3)-C(4)	125.2(3)
C(1)-S(1)-C(3)-S(2)	-1.0(2)
S(2)-C(3)-C(4)-C(8)	-0.3(5)
S(1)-C(3)-C(4)-C(8)	-123.2(3)
S(2)-C(3)-C(4)-C(5)	-177.8(2)
S(1)-C(3)-C(4)-C(5)	59.4(3)
C(6)-O(2)-C(5)-O(1)	175.8(3)
C(6)-O(2)-C(5)-C(4)	-4.3(5)
C(8)-C(4)-C(5)-O(1)	-176.3(3)
C(3)-C(4)-C(5)-O(1)	1.3(5)
C(8)-C(4)-C(5)-O(2)	3.8(5)
C(3)-C(4)-C(5)-O(2)	-178.6(3)
C(5)-O(2)-C(6)-C(9)	-177.6(3)
C(5)-O(2)-C(6)-C(7)	2.1(5)
C(9)-C(6)-C(7)-C(12)	1.9(5)
O(2)-C(6)-C(7)-C(12)	-177.7(3)
C(9)-C(6)-C(7)-C(8)	-179.6(3)
O(2)-C(6)-C(7)-C(8)	0.7(5)
C(5)-C(4)-C(8)-C(7)	-1.2(5)
C(3)-C(4)-C(8)-C(7)	-178.5(3)
C(6)-C(7)-C(8)-C(4)	-1.1(5)
C(12)-C(7)-C(8)-C(4)	177.1(3)
O(2)-C(6)-C(9)-C(10)	177.6(3)
C(7)-C(6)-C(9)-C(10)	-2.0(5)
C(19)-N(1)-C(10)-C(11)	-179.7(4)
C(17)-N(1)-C(10)-C(11)	3.2(5)

C(19)-N(1)-C(10)-C(9)	-1.0(5)
C(17)-N(1)-C(10)-C(9)	-178.0(3)
C(6)-C(9)-C(10)-N(1)	-178.3(3)
C(6)-C(9)-C(10)-C(11)	0.5(5)
N(1)-C(10)-C(11)-C(12)	179.9(3)
C(9)-C(10)-C(11)-C(12)	1.1(5)
C(10)-C(11)-C(12)-C(7)	-1.2(6)
C(6)-C(7)-C(12)-C(11)	-0.3(5)
C(8)-C(7)-C(12)-C(11)	-178.6(3)
C(14)-O(4)-C(13)-O(3)	-7.3(6)
C(14)-O(4)-C(13)-C(1)	167.8(3)
C(2)-C(1)-C(13)-O(3)	-143.3(4)
S(1)-C(1)-C(13)-O(3)	-17.7(5)
C(2)-C(1)-C(13)-O(4)	41.7(4)
S(1)-C(1)-C(13)-O(4)	167.3(2)
C(16)-O(6)-C(15)-O(5)	1.3(6)
C(16)-O(6)-C(15)-C(2)	178.6(4)
C(1)-C(2)-C(15)-O(5)	-14.3(5)
S(2)-C(2)-C(15)-O(5)	-134.9(4)
C(1)-C(2)-C(15)-O(6)	168.4(3)
S(2)-C(2)-C(15)-O(6)	47.8(4)
C(10)-N(1)-C(17)-C(18)	-91.3(4)
C(19)-N(1)-C(17)-C(18)	91.4(4)
C(10)-N(1)-C(19)-C(20)	-89.7(5)
C(17)-N(1)-C(19)-C(20)	87.6(5)

Symmetry transformations used to generate equivalent atoms:

Table 7. Hydrogen bonds for cd214397 [Å and °].

D-H...A	d(D-H)	d(H...A)	d(D...A)	<(DHA)
C(20)-H(20C)...S(2)#1	0.96	3.01	3.849(6)	147.0
C(9)-H(9)...O(1)#2	0.93	2.53	3.455(4)	173.9
C(2)-H(2)...O(3)#3	0.98	2.56	3.489(5)	158.2
C(20)-H(20C)...S(2)#1	0.96	3.01	3.849(6)	147.0
C(9)-H(9)...O(1)#2	0.93	2.53	3.455(4)	173.9
C(2)-H(2)...O(3)#3	0.98	2.56	3.489(5)	158.2
C(2)-H(2)...O(3)#3	0.98	2.56	3.489(5)	158.2
C(9)-H(9)...O(1)#2	0.93	2.53	3.455(4)	173.9
C(20)-H(20C)...S(2)#1	0.96	3.01	3.849(6)	147.0
C(2)-H(2)...O(3)#3	0.98	2.56	3.489(5)	158.2
C(9)-H(9)...O(1)#2	0.93	2.53	3.455(4)	173.9
C(20)-H(20C)...S(2)#1	0.96	3.01	3.849(6)	147.0

Symmetry transformations used to generate equivalent atoms:

#1 x,y-1,z #2 -x+2,y-1/2,-z+2 #3 -x+2,y+1/2,-z+1

References:

(1) Xuan, W. M.; Chen, C.; Cao, Y. T.; He, W. H.; Jiang, W.; Liu, K. J.; Wang, W. *Chem. Commun.* **2012**, *48*, 7292.

(2) Gerecke, M.; Brossi, A.; Friedheim, E. A. H. *Helv. Chim. Acta* **1961**, *44*, 955.

(3) Yuan, L.; Lin, W. Y.; Yang, Y. T. *Chem. Commun.* **2011**, *47*, 6275.

(4) Cory, A. H.; Owen, T. C.; Barltrop, J. A.; Cory, J. G. *Cancer Commun.* **1991**, *3*, 207.